Channel-Based Optimal Back-Off Delay Control in Delay-Constrained Industrial WSNs

Qihao Li, *Member, IEEE*, Ning Zhang, *Senior Member, IEEE*, Michael Cheffena, and Xuemin Shen, *Fellow, IEEE*

***Abstract*— Recent developments in industrial wireless sensor networks (IWSNs) have revolutionized industrial automation systems. However, harsh industrial environment poses great challenges to a time-critical and reliable wireless communication. For instance, effects of multipath fading, noise and co-channel interference can have unpredictable and time-varying impacts on the propagation channel, leading to the failure of on-time packet delivery. To address this problem, in this paper we propose a channel-based Optimal Back-off Delay Control (OBDC) scheme which can minimize the total time a packet spends in the sensor node (TSN) by assessing the features of a generic wireless channel. Specifically, we first explore the channel impairments by investigating the probability density function (PDF) of the level crossing rate (LCR) of the received signal in the industrial wireless environment. Then, with the obtained channel assessment results, we develop a phase-type semi-Markov model to investigate the probability distribution of the back-off delay of a packet in the sensor node (SN). The probability distribution of the back-off delay can be further substituted with TSN according to the queuing theory. The proposed OBDC scheme examines the Kullback-Leibler (KL) divergence between the obtained distribution of TSN and the packet arrival rate, and reduces the TSN according to an objective function which is constantly renewed in every transmission round with regard to a delay constraint. The simulation results show that the OBDC scheme can reduce TSN and guarantee to keep the TSN in an acceptable range even though the wireless channel is impaired by interference effects. It also shows that the OBDC scheme can reduce the proportion of packets meeting their deadline to the total packets in transmission when the number of SN and LCR changes.**

***Index Terms*— Industrial WSNs, level crossing rate, semi-Markov model, quadratic penalty method.**

I. Introduction

RECENT developments in industrial wireless sensor networks (IWSNs) have made revolutionary changes to the methods for information collection and analysis in the industrial automation. With sensor nodes (SNs) installed on industrial equipment, we can monitor parameters such as the actuator position, temperature and vibration to improve the efficiency of the production process as well as the public safety [1]–[3]. For example, in the packaging company "Polibol", the printing process during food packaging is performed by packing the food first and then printing the surface [4]. When sensors are installed to monitor the status of the ink in the outlet which dries up in a short time, the leakage can be prevented without polluting the food once the machines receive the monitoring report and close the outlet. However, to realize this envision, real-time data communication between SNs and actuators are required [5]–[8]. In addition, sensor data are typically time-sensitive in time-critical industrial applications. Since the packet of the demand response is only valid in a matter of milliseconds, the packets which arrive at their destinations later than their deadlines will be outdated and may adversely affect the performance of the target application. These cumulative effects of missing the deadline can degrade the efficiency of industrial production and thus cause an economic loss. To ensure the reliability of data transmission, the packet transmission delay must be controlled to meet critical service requirements throughout the manufacturing system.

However, it is challenging to fulfill the delay requirement for time-critical applications in the harsh industrial environment, especially to attain the appropriate total time a packet spends in the SN (TSN), which in this paper refers to the sojourn time a packet spends in the SN before the SN detects an idle channel status to access the propagation channel. First, the existing channel assessment method is unable to accurately evaluate the time-varying feature of the industrial propagation channel, and the incorrect channel assessment results can increase the packet collision probability, leading to the dramatic changes in the TSN. In the industrial environment, plenty of steel, metals and machinery are deployed around, which can produce multipath fading and interference effects to deteriorate the wireless propagation performance [3]. These fading dips can be far down below the proper threshold in a short period and degrade the strength of the received signal by as much as 30-40dB [5]. In order to prevent the unexpected degradation, signal to interference plus noise ratio (SINR) is accepted as a measurement of the channel quality in a plethora of research works. However, if SINR is applied to appropriate the channel quality during this period (without including the proper channel impairments for industrial environments),

Manuscript received August 31, 2018; revised February 20, 2019 and August 7, 2019; accepted October 6, 2019. Date of publication October 24, 2019; date of current version January 8, 2020. This work was supported in part by the Research Grant from the Regional Research Fund of Norway (RFF) and the Natural Science and Engineering Research Council (NSERC) in Canada. The associate editor coordinating the review of this article and approving it for publication was J. Liu. *(Corresponding author: Qihao Li.)*

Q. Li and M. Cheffena are with the Faculty of Engineering, Norwegian University of Science and Technology, N-2815 Gjøvik, Norway (e-mail: qihao.li@ntnu.no; micheal.cheffena@ntnu.no).

N. Zhang is with the Department of Computing Science, Texas A&M University-Corpus Christi, Corpus Christi, TX 78412 USA (e-mail: ning.zhang@tamucc.edu).

X. Shen is with the Department of Electrical and Computer Engineering, University of Waterloo, Waterloo, ON N2L 3G1, Canada (e-mail: sshen@uwaterloo.ca).

Color versions of one or more of the figures in this article are available online at http://ieeexplore.ieee.org.

Digital Object Identifier 10.1109/TWC.2019.2948156

the channel detection results obtained by the SN will be completely opposite to the actual ones. That is, when the busy channel is hampered by a burst of fading impairments, the SN will detect an idle channel status even though the channel is actually busy. The false detection result will inevitably lead to not only the loss of packet but also the channel congestion. In addition, the vibrating scatters and moving people bring changes to the phase and Doppler frequency of the received signal [9]. Rapid phase changes in each multipath component leads to destructive addition of the multipath components comprising the received signal, which in turn causes rapid variation in the received signal strength. Therefore, if the SNs are surrounded by machinery and workers, some conventional radio test method, e.g. SINR, may not be applicable to IWSNs. Second, conventional evaluation model may not be suitable to explore the delay performance of the Medium Access Control (MAC) protocol for current time-critical industrial applications. Specifically, in most cases, the packet sojourn duration in the conventional evaluation model is always described as a random variable which follows an exponential distribution. However, according to the IEEE 802.15.4 standard, the general MAC protocol suggests that the packet shall wait for a random back-off duration which follows a uniform distribution before attempting to access the channel. Hence, it is inappropriate to use the traditional evaluation model to build up an objective function for evaluating and optimizing the packet transmission delay. Third, the conventional IEEE 802.15.4 standard may fail to react promptly to sudden changes in the wireless channel and thus increase the TSN. As the protocols are designed mainly for uncritical operation, they cannot respond to the time-varying wireless channel in a timely manner. Moreover, the SNs set the back-off waiting time of each packet based on the failure times of the SNs to detect an idle channel status. Therefore, it is difficult to reduce the TSN by adjusting the waiting time of a packet based on a predesigned protocol in the time-varying industrial environment.

To adaptively control the TSN based on the channel assessment results for industrial applications, we develop a channel-based packet transmission delay optimal control scheme, called Optimal Back-off Control (OBDC) scheme, with an aim to minimize the TSN for the IWSNs. Explained in more detail, in order to reduce the channel false detection rate and achieve statistically consistent channel status, we produce a probability density evaluation model by investigating the probability density function (PDF) of the level crossing rate (LCR) of a transmission signal passing through a pre-determined threshold in the industrial wireless channel. Then, we develop a semi-Markov model and substitute the obtained channel detection result into this model to study the packet sojourn duration which follows a uniform distribution. Finally, we produce a constantly updated objective function to optimize the back-off delay with barrier penalty method in a given TSN constraint. Preliminarily, we have proposed a sampling rate and queuing state control (CSQC) scheme [4] to minimize the TSN for IWSNs in the light of the information of channel state and queuing state. Although the CSQC scheme can control the packet transmission delay by updating the data sampling rate according to the instantaneous information of the channel state and the packet queuing state, the scheme overlooks the impact of the distribution characteristics of the packet sojourn distribution. The CSQC scheme also fails to consider the delay constraint and thus is unable to meet the industrial application requirements.

Specifically, the main contributions of this paper are as follows.

- **First**, we design a trigonometry decomposition method to investigate the PDF of LCR. And also note that the PDF of LCR can be expressed as the multiplication between the combination of the power gain and frequency angular of the multipath received signal with the interference effects and the PDF of the corresponding multipath received signal. Moreover, when the obtained instantaneous probability of the PDF of LCR falls outside the confidential interval, the SN can determine the channel quality as the opposite status compared with the detected one.
- **Second**, we design a semi-Markov model for the OBDC scheme in which the variable of the packet sojourn state follows a uniform distribution. A phase-type transition model is used as the embedded Markov chain of the semi-Markov model. Specifically, in contrast to a general embedded Markov model, a phase-type model can simplify the expression of the final objective function in the OBDC scheme. Additionally, by considering the obtained PDF of LCR as the transition probability, we explore the probability distribution of the time interval between the SN setting the back-off delay of the packet and the SN successfully detecting an idle channel status. The obtained probability distribution is used to construct the final objective function.
- **Third**, by calculating the Kullback-Leibler (KL) divergence of the probability distribution between the TSN and inter-arrival time of each packet in the SN, we propose a back-off control scheme to minimize the TSN. In contrast to other back-off control schemes, the OBDC scheme can constantly change the objective function of the TSN according to the obtained PDF of LCR and the times of SN failing to detect a free channel status. By constructing the objective function subject to the delay constraints, we calculate the back-off delay descent direction and further find the optimal delay steps to obtain the optimal back-off delay for the packets.

The remainder of this paper is organized as follows. The related works are presented in Sec. II. The system model and problem formulation are introduced in Sec. III. Sec. IV describes the OBDC scheme. Simulation results are shown in Sec. V. Finally, conclusions are given in Sec. VI.

II. Literature Review

A plethora of research efforts have been made on optimizing the TSN for conventional sensor networks with delay constraint [6], [10]–[12]. The proposed control schemes in optimizing the packet transmission delay can be briefly divided into three categories: the equivalent-rate constraint

approach [6], the Lyapunov stability drift approach [11] and the approximate Markov decision process approach [12].

In the equivalent-rate constraint approach, most works control the TSN by analyzing a delay objective function subject to delay constraints. Specifically, all these schemes convert the delay constraints into the average packet arrival rate on the basis of the large deviation theory. For example, [6] considers the limitation on the packet transmission delay and applies the delay constraints to the optimal link scheduling problems. Specifically, [6] produces a mixed-integer optimization function, which is formulated based on the knowledge of the weighted effective capacity of each transmission link dependent on the data rate constraints derived from the delay information. Similarly, the achievable throughput and delay performance of multiple access channels are studied in [13] by jointly employing the limitation on the buffer overflow probability and effective transmission rate (modified by delay bound). However, there is a premise for the performance of all these schemes, that is the working environment of the network should be free of harsh multipath fading and interference effects, which is impossible in the industrial environment. In the Lyapunov drift approach, the analysis of the delay optimization problem is shifted to analyze the stability characteristics of the system according to the Lyapunov drift method with delay constraints. [11] proposes a modified max-weight queue control policy to achieve queuing stability and satisfy delay constraint. Likewise, [11] applies the Foster-Lyapunov criteria to the proposed control policy in order to hold steady packet delay. In [14], a multi-objective function is produced to mitigate the delay and energy-hole problem. Considering the Lyapunov drift approach, [14] builds up a lifetime maximization scheme based on the multi-objective function in terms of the network connectivity and latency. Neely *et al.* [15] investigates the joint stability and utility optimization in a multiuser one-hop wireless system. A delay-based Lyapunov function is used to address the challenge of time-varying reliability and stringent requirement of the packet transmission delay. The approach is further introduced in [16] that the Lyapunov drift and Lyapunov optimization theory are used to solve the max-weight queuing problem bound by the delay constraints [16]. As the performance of this approach depends on the pre-designed schedules to control the medium access, it cannot update the objective function frequently to adapt to the time-varying industrial environment. Thus, it cannot be directly applied to the industrial applications. The Markov decision process resolves the delay optimization problem by characterizing the system state with both channel and queuing state information. Lei *et al.* [12] proposes an average reward constraint Markov decisions model to optimize the lifetime of sensors under the delay constraint while minimizing the weighted packet loss rate in the IWSNs. The deterministic Markov decision model is also employed to minimize the average end-to-end delay in a device-to-device network limited to the constraint of packet dropping probability [17]. In these conventional evaluation models, the packet sojourn duration is described as a random variable which follows an exponential distribution. However, as explained in the last section, the packet back-off duration should follow a uniform distribution. Therefore, conventional Markov decision model may be incapable of evaluating the delay performance and not suitable for building up the objective function of the packet transmission delay for extra control and optimization in the industrial environment.

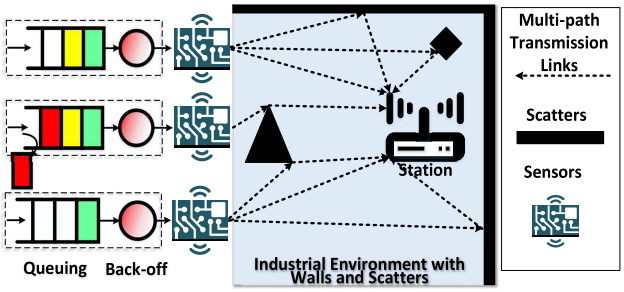

Fig. 1. Network model.

In a word, the effect of the propagation impairments in the harsh industrial environment can decrease the accuracy of the equivalent-rate constraint approach, while the predesigned medium access of the control schemes makes it difficult for the SNs to adapt to the time-varying propagation channel in the Lyapunov drift approach, and the failure of the conventional Markov decision model to correctly describe the packet sojourn duration distribution means that it cannot be directly applied to the IWSNs. In order to address these challenges, we develop an OBDC scheme to minimize the TSN in IWSNs.

III. System Model and Problem Formulation

A. Network Model

In this paper, we consider an IWSNs system, which operates in a harsh industrial environment filled with signal scatters, which are uniformly deployed in this scenario. These scatterers are consisted by various kinds of materials. The transmitted signal is reflected from the scatterers causing heavy multipath propagation that impair the received signal. As shown in Fig. 1, the network consists of two primal components: base station (**BS**) and **SNs**. BS is used to allocate the network resources and manage the data transmission of the SNs. Versatile SNs are uniformly deployed in the place of interest to perceive and measure the surrounding environment [18], [19]. The SNs store the measurement data into their memory, queue the packets (following first-come-first-serve principle), and transmit the packets while detecting an idle channel status. The BS and SNs communicate with each other according to the IEEE 802.15.4 standard. The network follows star topology, which connects all the SNs and the BS within one hop.

B. LCR in the Industrial Environment

As aforementioned, SINR cannot be directly applied to the control scheme in IWSNs. In this section, we introduce the PDF of LCR, which refers to the threshold crossing probability of the received signal per time unit, to explore the industrial channel features and improve the channel assessment ability of the SN. Let R be the given signal crossing threshold. Then, the

PDF of LCR, which is denoted by $L_r(R)$, refers to the PDF of the received signal crossing R in a positive direction [5]. Thus, the expression of the PDF of LCR can be given as, $L_r(R) = \mathbf{d}t \int_0^\infty \dot{r} p_{r\dot{r}}(R, \dot{x}) d\dot{x}$, where $R \geq 0$ and $p_{r\dot{r}}(x, \dot{x})$ is the joint density function of the received signal and its time derivative $\dot{r}(t)$ at the same time instant. Let $s(t) = p \exp(jwt)$ be the transmitted signal, where p is transmission power gain, w is the angular frequency and t is the related time instant. We assume that the signal is transmitted in a line of sight propagation scenario (there is a direct predominant path over the indirect ones) and influenced by multipath fading and co-channel interference from the neighboring SNs. The received signal is then expressed as $r(t) = p_0 \exp(jw_0 t) + \sum_n p_n \exp(jw_n t + \theta_n)$, where p_0 and w_0 are the prominent received power gain and angular frequency; p_n and w_n are the power gain and angular frequency received from the nth reflection path. Let $G(t) = \sum_n G_n \exp(jv_n t)$ be the co-channel interference effects, where G_n and v_n are the interference power gain and the angular frequency the on the nth path. Let $K = r(t)/G(t)$ be the signal-to-interference-ratio. Considering the signal-to-interference-ratio, which builds up the relationship between the received multi-path signal and interference effects, the joint received signal, which consists of multipath signals and interference effects, can be expressed as

$$\begin{aligned} f(t) &= r(t) - KG(t) \\ &= p_0 \exp(jw_0 t) + \sum_n p_n \exp(jw_n t + \theta_n) \\ &\quad - K \sum_n G_n \exp(jv_n t) \\ &= Q + \left(\sum_n p_n \cos(w_n t + \theta_n) - \sum_n g_n \cos(v_n t) \right) \\ &\quad - j \left(\sum_n p_n \sin(w_n t + \theta_n) - \sum_n g_n \sin(v_n t) \right) \end{aligned} \tag{1}$$

where $g_n = KG_n$, $Q = p_0 \exp(jw_0 t)$. A trigonometry decomposition method is proposed to find out the density function of $f(t)$ (see Appendix A for details). After some algebraic manipulation, we calculate out the numerical result of the PDF of LCR in the industrial environment, which can be written as (see Appendix A for details)

$$L_r(R) = \mathbf{d}t \int_0^\infty \dot{r} p_{r\dot{r}}(R, \dot{x}) d\dot{x} = \mathbf{d}t N_r(R) \tag{2}$$

where $N_r(R)$ is the LCR of the received signal. We find that the PDF of LCR is proportional to the PDF of the received signal. The proportional constant is determined by not only the power gain of the multi-path signal and the interference effects, but also the difference between their angular frequency.

In short, LCR allows more direct insights into channel quality with an immediate interpretation which describes the occurrence rate of fading dips. Likewise, the PDF of LCR can be used to detect the probability of the received field strength crossing the detected signal power in the positive direction. To do this, the received signal strength is first substituted into the PDF of LCR. When the obtained instantaneous probability falls outside the confidential interval, the SN can determine that the channel quality is opposite to previously detected channel status. For example, when the channel meets an abrupt fading dip in a busy channel, the SN can estimate the channel quality by calculating the PDF of LCR with the received signal power at current time instant. If the probability falls inside the confidential interval, it means that the channel is impaired by heavy fading during this interval; otherwise, the channel quality is clear for packet transmission.

C. Phase-Type Semi-Markov Model

In this single-hop IWSNs, we assume that all the SNs are synchronized and they are capable to detect the channel status during clear channel assessment (CCA) slots [20]. We assume that all the packets in the MAC layer are with the same fixed length. Besides, we assume that the SN can successfully transmit the packets if it detects an idle channel status. Furthermore, we don't consider the acknowledgement from link layer. Thus, after N attempts, if the SN still cannot detect an idle channel, it will discard the old packet, prepare a new one and restart the CCA procedure. Accordingly, in this part, we investigate the probability distribution of the contention access period in the SN.

According to the IEEE 802.15.4 standard [21], for each transmission round, the SN first waits for *Backoff* delay specified by back-off exponential (*BE*), which is uniformly initiated in the range of $[1, 2^{BE} - 1]$. Then, it performs the first CCA, i.e., it senses the channel, and if it is idle, the first CCA succeeds, and number of contention times (*CW*) is decreased by 1. The SN then performs the second CCA, and if it is also successful, then it can transmit the packet. If either of the CCAs fails, both number of back-off times (*NB*) and *BE* are incremented by 1, ensuring that *BE* levels at *macMaxBE*, and *CW* is reset to 2. The SN repeats the procedure for the new back-off stage by drawing a new back-off value, unless the value of *NB* becomes greater than *macMaxCSMABack-offs* [21]. In that case, the CSMA/CA algorithm terminates with a channel access failure status, and discards the packet.

In the following part, we explore the probability distribution of the interval between the SN setting the back-off delay of the packet and the SN successfully detecting an idle channel status to transmit the packet. Considering that the back-off delay of the packet follows uniform distribution, we build up the connection between each back-off state based on semi-Markov model. In addition, we define the transition probability of the embedded Markov chain in the semi-Markov model as the LCR of the received signal. The reason is that, according to the description of the standard, NB is increased only if the SN detects a busy channel status, which refers to the SN finds the received signal is beyond the given threshold. Thus, we can refer to the transition probability as the PDF of LCR in a given threshold at the time instant Δt. Denote by $\mathbb{N}_+ = 1, 2, \ldots$, $\mathbb{N} = \mathbb{N}_+ \cup \{0\}$ the time scale and $\mathbb{E}$ the finite state space in the proposed semi-Markov model. Note that space $\mathbb{E}$ contains all the back-off states and the total number of the states in $\mathbb{E}$ is defined by *macMaxCSMABack-offs* according to the

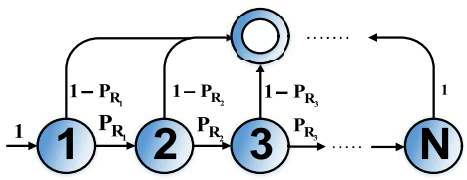

Fig. 2. Phase-type embedded Markov chain.

CSMA/CA algorithm. Additionally, denote by $T = (T_n)_{n\in\mathbb{N}}$ the successive time instants when state changes in $\mathbb{E}$ and $X = (X(T_n)) = (X_n)_{n\in\mathbb{N}}$ the successively visited states before T_n. Let $S = (S(T_n)) = (S_n) \in \mathbb{E}$ be the *NB*-th back-off state in $\mathbb{E}$ at T_n. Set $\tau = (\tau_n) = (T_n - T_{n-1})_{n\in\mathbb{N}_+}$ for the successive sojourn time in X_n. Considering the transition state and the time instant, the Markov renew chain can be denoted by $(X, T) = (X_n, T_n)_{n\in\mathbb{N}} = (S_n, T_n)_{n\in\mathbb{N}}$.

Fig. 2 shows the proposed phase-type embedded Markov model. According to IEEE 802.15.4, when *NB* is increased to *macMaxCSMABack-offs*, whether the packet is successfully transmitted or discarded, this packet should be always removed from the back-off state. After that, a new packet will occupy the back-off state of the old one. Thus, we refer to the state that a new packet occupy the old one as the absorption state of the phase-type embedded Markov model. Denote by $P_{R,n}$ the probability of detecting a busy channel at X_n state conditioned on the level crossing threshold R. Then, making use of the pre-defined PDF of LCR $L_r(R) \to P_{R,n}$, the transition probability between the states in the phase-type embedded Markov chain can be referred to $p_{S_{n+1},S_n} = P_{R,n} = \int_0^\infty p(R,\dot{R})d\dot{R}$, where $S_n, S_{n+1} \in \mathbb{E}$. Denote by $\boldsymbol{p}$ the transition matrix of the phase-type embedded Markov model

$$\boldsymbol{p} = \left(\begin{array}{ccccc:c} -P_{R,1} & P_{R,1} & 0 & \dots & 0 & 1-P_{R,1} \\ 0 & -P_{R,2} & P_{R,2} & \dots & 0 & 1-P_{R,2} \\ \vdots & \vdots & \vdots & \vdots & \vdots & \vdots \\ 0 & 0 & 0 & 0 & -1 & 1 \\ \hdashline 0 & 0 & 0 & 0 & 0 & 0 \end{array}\right) \tag{3}$$

The sojourn time of state S_n is the amount of back-off delay that passes before making a state transition. Relaxing these constraints yields a semi-Markov process that operates in the following fashion. **1)** After entering state S_n, the process selects its next state $n+1$ according to the phase-type embedded Markov model. **2)** The back-off time spent in state S_n before jumping into next state S_{n+1} is given by τ_n which follows uniform distribution.

Let $F_{S_{n+1},S_n}(t)$ be the sojourn time distribution in a given state S_{n+1} conditioned on coming from state S_n. According to the standard, $F_{S_{n+1},S_n}(t)$ in state S_{n+1} conditioned on S_n follows uniform distribution

$$\begin{aligned} F_{S_{n+1},S_n}(t) &= P\{T_{n+1} - T_n \le t | X_{n+1} = S_{n+1}, X_n = S_n\} \\ &= \begin{cases} 0, & t < 1 \\ \dfrac{t-1}{2^{\mathrm{BE}+i-1}-1}, & 1 \le t < 2^{\mathrm{BE}+i-1} \\ 1, & t \ge 2^{\mathrm{BE}+i-1} \end{cases} \end{aligned} \tag{4}$$

Additionally, the PDF and the complementary cumulative distribution function (CCDF) are shown as below.

1) If system stays at the initial state, the CCDF is given by

$$f_{S_n,0}(t)dt = P\{t < T_0 < t + \Delta t | X_0 = S_n\} \tag{5}$$

$$\bar{F}_{S_n,0}(t)dt = P\{T_0 > t | X_0 = S_n\} = \int_t^\infty f_{S_n,0}(x)dx \tag{6}$$

2) If system stays at S_n conditioned on coming from S_{n-1}

$$\begin{aligned} f_{S_n,S_{n-1}}(t)dt &= P\{t < T_n < t \\ &\quad + \Delta t | X_n = S_n, X_{n-1} = S_{n-1}\} \\ \bar{F}_{S_n,S_{n-1}}(t)dt &= P\{T_n > t | X_n = S_n, X_{n-1} = S_{n-1}\} \\ &= \int_t^\infty f_{S_n,S_{n-1}}(x)dx \end{aligned} \tag{7}$$

Let $\mathbf{q}$ be the kernel of the associate discrete time semi-Markov model

$$\mathbf{q} = \{q_{S_n,S_{n-1}}(t); S_n, S_{n-1} \in \mathbb{E}, t \ge 0\} \tag{8}$$

where

$$\begin{aligned} &q_{S_n,S_{n-1}}(t) \\ &= \lim_{\Delta t \to 0} \frac{P\{X_n = S_n, t < T_n \le t + \Delta t | X_{n-1} = S_{n-1}\}}{\Delta t} \end{aligned} \tag{9}$$

Therefore, the probability that state S_{n-1} transit to state S_n during $(t, t+\Delta t)$ conditioned on staying at S_n at time t can refer to $q_{S_n,S_{n-1}}\Delta + o(t)$. The equation of $q_{S_n,S_{n-1}(t)}$ in (8) implies that

$$\begin{aligned} &P\{X_n = S_n, t < T_n \le t + \Delta t | X_{n-1} = S_{n-1}\} \\ &\quad = P\{t < T_n \le t + \Delta t | X_n = S_n, X_{n-1} = S_{n-1}\} \\ &\qquad \cdot P\{X_n = S_n | X_{n-1} = S_{n-1}\} \end{aligned} \tag{10}$$

Then, we rewrite the transition probability of the semi-Markov kernel as

$$\begin{aligned} &q_{S_n,S_{n-1}}\Delta t + o(\Delta t) \\ &\qquad = f_{S_n,Sn-1}(t)p_{S_n,S_{n-1}}\Delta t + o(\Delta t) \end{aligned} \tag{11}$$

In this part, we are interested in the probability that the packet comes into the absorption state at time t conditioned on coming from the nth back-off state of the SN. Let $U_{S_N,S_n}(t)$ be the probability being in state S_N at time t conditioned on coming from state S_n, that is

$$U_{S_N,S_n}(t) = P\{X(T_N) = S_N, T_N > t | X(T_0) = S_n\} \tag{12}$$

Moreover, let $w_{S_m,S_n}(\tau)d\tau$ be the probability that system leaving state S_m during $(\tau, \tau + d\tau)$ conditioned on coming from state S_n, that is

$$\begin{aligned} &w_{S_m,S_n}(\tau)d\tau \\ &\quad = P\{X(T_n) = S_m, t < T_n \le t + dt | X(T_0) = S_n\} \end{aligned} \tag{13}$$

The probability $U_{S_N,S_n}(t)$ in the absorption state at time t conditioned on coming from state S_n is given by

$$\begin{aligned} U_{S_N,S_n}(t) &= \bar{F}_{0,S_n}(t)\delta_{S_N,S_n} \\ &\quad + \sum_{\substack{S_m \in \mathbb{E} \\ m > n}} p_{S_N,S_m} \int_0^t w_{S_m,S_n}(\tau)\bar{F}_{S_N,S_m}(t-\tau)d\tau \end{aligned} \tag{14}$$

Shift the problem into the Laplace domain, then the convolution of two functions can be transferred to the product of these functions. Another important advantage of working with Laplace transforms is that we can derive arbitrary moments of $U_{S_N,S_n}(t)$ and $w_{S_m,S_n}(t)$ by derivatives of each Laplace domain function at $s=0$. By taking Laplace transform into account, we can obtain that

$$U^*_{S_N,S_n}(s) = \bar{F}^*_{0,S_n}\delta_{S_N,S_n} + \sum_{\substack{S_m\in\mathbb{E}\\ m>n}} p_{S_N,S_m} w^*_{S_m,S_n}(s)\bar{F}^*_{S_N,S_m}(s) \tag{15}$$

$$w^*_{S_m,S_n}(s) = f^*_{0,S_n}\delta_{S_m,S_n} + \sum_{\substack{S_m,S_n\in\mathbb{E}\\ m>n}} p_{S_m,S_{m-1}} w^*_{S_{m-1},S_n}(s) f^*_{S_m,S_{m-1}}(s) \tag{16}$$

Due to the specific type of problem and the corresponding embedded Markov model, there is only one state could be selected if it doesn't transit into the absorption state. Therefore, $w^*_{S_m,S_n}(s)$ and $U^*_{S_N,S_n}(s)$ can be simplified as

$$w^*_{S_m,S_n}(s) = \prod_{n}^{m-1} p_{S_{n+1},S_n} f_{S_{n+1},S_n}(s)$$

$$\begin{aligned} U^*_{S_N,S_n}(s) &= p_{S_N,S_n}\bar{F}_{S_N,S_n}(s) + \sum_{m=n+1}^{N-1} p_{S_N,S_m} w^*_{S_m,S_n}(s)\bar{F}_{S_N,S_m}(s) \\ &= p_{S_N,S_n}\bar{F}_{S_N,S_n}(s) + \sum_{m=n+1}^{N-1} p_{S_N,S_m}\left(\prod_{n}^{m-1} p_{S_{n+1},S_n} f_{S_{n+1},S_n}(s)\right) \bar{F}_{S_N,S_m}(s) \end{aligned} \tag{17, 18}$$

Denote by x_n the practical back-off delay spent in state S_n. According to the aforementioned PDF and CCDF of the sojourn time distribution, we have the expression of $f_{S_n,S_{n+1}}(s)$ and $\bar{F}_{S_m,S_N}(s)$ as

$$\begin{aligned} f_{S_{n+1},S_n}(s) &= \int_0^\infty e^{-st}\frac{1}{x_n}dt = \frac{1}{x_n s} \\ \bar{F}_{S_N,S_m}(s) &= \int_0^\infty e^{-st}\frac{t}{x_n}dt = \frac{1}{x_n s^2} \end{aligned} \tag{19}$$

Substitute (19) into (17), then we have

$$U_{S_N,S_n}(s) = P_{S_N,S_n}\frac{1}{x_n s^2} + \sum_{m=n+1}^{N-1} p_{S_N,S_m}\left(\prod_{n=i}^{m-1} p_{S_{n+1},S_n}\frac{1}{x_{n+1}s}\right)\frac{1}{x_n s^2} \tag{20}$$

Simplifying and taking Laplace inverse transform of (20), we have

$$U_{N,n}(t) = \left(\frac{p_{N,n}}{x_n} + \frac{p_{N,n+1}p_{n+1,n}}{x_{n+1}x_n} + \cdots + \frac{p_{n+1,n}p_{n+2,n+1}\cdots p_{N,N-1}}{x_n x_{n+1}\cdots x_N}\right)t + O(t^2) \tag{21}$$

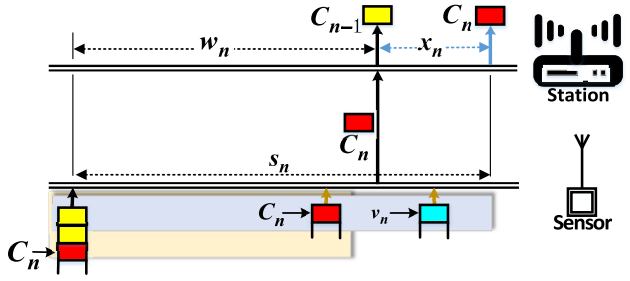

Fig. 3. Total time a packet spent in the SN.

where we define $p_{n+1,n} = p_{S_{n+1},S_n}$. Considering $e^t \approx 1+t+\frac{t^2}{2!}+\cdots$, $U_{N,n}(t)$ can be further simplified as $e^{U(t)}$ instead. In the next section, the TSN optimization is discussed. According to the queuing theory [22], it can be a good choice to let the TSN have the similar probability distribution with the packet interarrival time distribution. This can be the reason on why the system can still keep stable while the back-off delay is increased by 2^i. Now we have obtained the expression of the time from the sensor setting the back-off delay of the packet to the sensor successfully detecting an idle channel status to transmit the packet.

D. KL Divergence Between the TSN and Packet Arrival Rate

Suppose that the arriving packets which are generated by the sensed data, follow a Poisson model. The interarrival time distribution of each packet is given by $A(t) = 1-e^{-\lambda t}, t \geq 0$ with an average arrival rate of λ packets per second [23]. According to the MAC model, when the packet comes to back-off state, it will be hold at the head of the queue until it detects an idle channel status. We assume this packet sojourn interval when the packet stays at the head of the queue as the packet service interval. Fig. 3 shows the time spent in the SN for the nth packet entering into the queue. We denote this nth packet by C_n. We define the TSN for C_n as x_n and the PDF of x_n as $P(x_n < x) = B(x)$. The interval w_n denotes the waiting time of C_n in the queue for all the packets ahead being sent. We define it as the waiting time in queue for packet C_n. The TSN, C_n, in the SN is the sum of its waiting time and service time, which we denote by $s_n \triangleq$ system time for $C_n = w_n + x_n$. Let q_n be the number of packets left behind by departure of C_n from service. Let v_n be the number of packets arriving during the service of C_n. In addition, taking v_n as an example, we introduce the limiting principle, which is defined as $\tilde{v} \triangleq \lim_{n\to+\infty} v_n$ [24]. We define the z transform for $\tilde{v}$ as $V(z) \triangleq E[z^{\tilde{v}}] \triangleq \sum_{k=0}^{\infty} P[\tilde{v}=k]z^k$. As shown in Fig. 3, v_n, the number of arrivals during x_n depends only upon the duration of x_n. By the law of total probability, we further have

$$\begin{aligned} V(z) &= \sum_{k=0}^{\infty}\int_0^\infty P[\tilde{v}, x < \tilde{x} \leq x+dx]dx z^k \\ &= \sum_{k=0}^{\infty}\int_0^\infty \frac{(\lambda x)^k}{k!}e^{-\lambda x}b(x)dx z^k \\ &= \int_0^\infty e^{-(\lambda+\lambda z)x}b(x)dx \end{aligned} \tag{22}$$

We define the Laplace transfer $B(s)$ for $b(x)$ as $B(s) \triangleq \int_0^\infty e^{-sx} b(x)dx$. Replacing s by $\lambda - \lambda z$ and substituting the result of (22) into $B(s)$ we have $V(z) = B(\lambda - \lambda z)$. It reflects the relationship between the number of arrivals $\tilde{v}$ occurring during the service interval $\tilde{x}$ where the arrival process is Poisson process.

Now consider q_n, the number of packets left behind by the departure of C_n. In Fig. 3, we see that q_{n+1} equals to q_n less 1 plus the number of packets that arrive during the service interval x_{n+1}. Thus, we have $q_{n+1} = q_n - \Delta q_n + v_{n+1}$, where

$$\Delta q_n = \begin{cases} 1 & q_n = 1, 2, \dots \\ 0 & q_n = 0. \end{cases} \tag{23}$$

Then explore the relationship between the z-transform for the probability of finding k packets in the system and the number of arrival packets during service time [25]. We define the z-transform for q_n as $Q_n(z) \triangleq \sum_{k=0}^{\infty} P[q_n = k] z^k$. Considering limiting principle we have

$$Q(z) = \lim_{n \to +\infty} Q_n(z) = \sum_{k=0}^{\infty} P[\tilde{q} = k] z^k = E[z^{\tilde{q}}] \tag{24}$$

Substituting q_n into $Q_n(z)$, the expression of $Q(z)$ is expressed as

$$Q(z) = V(z) \frac{P[\tilde{q} = 0](1 - 1/z)}{1 - V(z)/z} \tag{25}$$

Considering a first-come-first-served system, those packets present upon the arrival of C_n must depart before it does. Moreover, those packets that C_n leaves behind must be precisely those who arrive during its stay in the SN. Thus, referring to Fig. 3, we may identify those packets who arrive during the time interval s_n as being our previously defined q_n. Under the condition of Poisson arrival process at rate λ packets per second, v_n, the number of arrivals during the interval whose duration is x_n is analogous to q_n, and the number of arrivals during the interval whose duration is s_n. Since v_n is analogous to q_n, then $V(z)$ must be analogous to $Q(z)$. Similarly, since x_n is analogous to s_n, then $B(s)$ must be analogous to $S(s)$. Then, we have direct analogy from the definition of $V(z)$ that $Q(z) = S(\lambda - \lambda z)$. Replace $\lambda - \lambda z$ by s, then we have expression for $S(s)$ as

$$S(s) = B(s) \frac{sP[\tilde{q} = 0]}{s - \lambda + \lambda B(s)} \tag{26}$$

Taking expectation of both sides of q_n, it yields that $E[q_{n+1}] = E[q_n] - E[\Delta_{q_n}] + E[v_{n+1}]$. Then taking the limiting principle as $n \to \infty$, we have $E[\tilde{q}] = E[\tilde{q}] - E[\Delta_{\tilde{q}}] + E[\tilde{v}]$, which yields $E[\Delta_{\tilde{q}}] = E[\tilde{v}]$. From the definition in (23), we rewrite $E[\Delta_{\tilde{q}}]$ as

$$\begin{aligned} E[\Delta_{\tilde{q}}] &= \sum_{k=0}^{\infty} \Delta_{\tilde{q}} P[\tilde{q} = k] \\ &= \Delta_0 P[\tilde{q} = 0] + \Delta_1 P[\tilde{q} = 1] + \Delta_2 P[\tilde{q} = 2] + \cdots \\ &= 0 \cdot P[\tilde{q} = 0] + 1 \cdot P[\tilde{q} > 0] \\ &= P[\tilde{q} > 0] = P[\text{busy system}] \end{aligned} \tag{27}$$

From the definition of utilization factor, we have $P[\text{busy system}] = \rho = \lambda \bar{x}$. Making this change of ρ in (26), it yields that

$$S(s) = B(s) \frac{s(1 - \rho)}{s - \lambda + \lambda B(s)}, \tag{28}$$

which is the expression of the Laplace transform of the distribution of $\tilde{s}$, TSN. Taking inverse Laplace transform of (26), we can obtain the PDF for $\tilde{s}$.

The objective of this paper is to minimize $\tilde{s}$, the TSN, such that the packet can be forwarded to the base station in time. In this part, we explore the optimal condition of the service schedule method to guarantee that $\tilde{s}$ is below the threshold. Let $p(x|\mu)$ be the expected distribution of $\tilde{s}$ conditioned on parameter μ. Denote by $q(x; b(x))$ the distribution of $\tilde{s}$. We use Kullback-Leibler (KL) divergence ($\mathcal{KL}(\cdot\|\cdot)$) to measure how $q(x; b(x))$ diverges to $p(x|\mu)$. In order to find the optimal parameter of $q(x; b(x))$ which can achieve similar statistical performance with $p(x|\mu)$, we minimize the KL convergence with respect to $b(x)$,

$$\begin{aligned} b^*(x) &= \underset{b(x)}{\operatorname{argmin}} \mathcal{KL}\left(p(x|\mu) \| q(x; b(x))\right) \\ &= \underset{b(x)}{\operatorname{argmin}} \mathbb{E}_{p(x|\mu)} \left[\log p(x|\mu) - \log q(x; b(x))\right] \end{aligned} \tag{29}$$

Taking derivative of (29) on $b(x)$, we have

$$\begin{aligned} &\nabla_{b(x)} \mathcal{KL}\left(p(x|\mu) \| q(x; b(x))\right) \\ &\qquad = \nabla_{b(x)} - \mathbb{E}_{p(x|\mu)} \left[\log q(x; b(x))\right] \end{aligned} \tag{30}$$

(30) indicates that $q(x; b(x))$ has a significant impact on the optimal value $b^*(x)$. As the Laplace transform of $p(x|\mu)$ and $q(x; b(x))$ keeps its original convexity feature, we have

$$\begin{aligned} &\underset{b(x)}{\operatorname{argmin}} \mathcal{KL}\left(p(x|\mu) \| q(x; b(x))\right) \\ &\quad \Leftrightarrow \underset{b(x)}{\operatorname{argmin}} - \sum_x p(x|\mu) \log q(x; b(x)) \\ &\quad \overset{\mathcal{F}}{\Leftrightarrow} \underset{\mathcal{F}\{b(x)\}}{\operatorname{argmin}} - \sum_s \mathcal{F}\{p(x|\mu)\} \mathcal{F}\{\log q(x; b(x))\} \\ &\quad \Leftrightarrow \underset{B(s)}{\operatorname{argmin}} - \sum_s p(s|\mu) \log S(s; B(s)) \end{aligned} \tag{31}$$

Based on (31) and (26), if we want to minimize the convergence gap between $p(x|\mu)$ and $q(x; b(x))$, one of the optimal methods is to make $B(s)$ closer to the packet arrival rate λ. This relationship between the service rate and arrival rate is also proved in queuing theory.

E. Problem Formulation

Our objective is to minimize the TSN by adjusting the back-off delay according to the channel status. Suppose $U_{N,n}(t; x_n)$ can be approximated as $\exp[t(\ln p_n x_n + \ln p_n p_{n+1} x_n x_{n+1} + \dots)]$. In this scheme, we do not try to predict the channel status in next back-off round. Instead, we consider that all the channel status in the future back-off round have the same channel status. The reason is that, from one side, it consumes too many computational resource to do prediction; from the other side, the new back-off delay

is obtained from the new objective function in the next transmission cycle. Therefore, we can simplify $U_{N,n}(t;x_n)$ as $\exp[t(\ln p_n x_n + \ln p_n^2 x_n x_{n+1} + \ldots)]$. Let $A(t) = \exp(-\lambda t)$ be the arrival distribution, where λ is the packet arrival rate. As aforementioned, if we want to minimize the TSN, one of optimal methods is to minimize the KL divergence between the average packet sojourn distribution and arrival distribution bound by the back-off delay. According to (31) and (21), we have

$$\begin{aligned}&\underset{x_n}{\operatorname{argmin}}\ \mathcal{KL}\left(A(t)\|U_{n,N}(t;x_n)\right)\\ &\Leftrightarrow \underset{x_n}{\operatorname{argmin}}\ \sum_t e^{-\lambda t}\log\left(\frac{e^{-\lambda t}}{e^{t(\ln p_n x_n+\ln p_n^2 x_n x_{n+1}+\ldots)}}\right)\\ &\Leftrightarrow \underset{x_n}{\operatorname{argmin}}\ \ln p_n x_n + \ln p_n^2 x_n x_{n+1} + \ldots - \lambda \end{aligned} \tag{32}$$

In our scheme, the algorithm makes a new back-off delay by choosing a direction d_n and searching along this direction for α_n distance from the current back-off delay x_n. The iteration is given by $x_{n+1} = x_n + \alpha_n d_n$. where positive scalar α_n is called the step size, d_n is the direction which guarantees that the objective function $\mathcal{KL}\left(A(t)\|U_{n,N}(t;x_n)\right)$ can be reduced along this direction. In addition, due to the delay constraint, we have $x_0+x_1+\cdots x_n \le T$, where T is a pre-defined packet valid delay. Combine (32), x_{n+1} and the constraint condition, then we have the objective function at the nth transmission round, that is

$$\begin{aligned}&\underset{x_n}{\operatorname{argmin}}\ \ln p_n x_n + \ln p_n^2 x_n x_{n+1} + \ldots - \lambda\\ &\text{s.t. } x_{n+1} = x_n + \alpha_n d_n,\\ &\quad \sum_n x_n < T,\ x_n > 0, \alpha > 0, \quad \forall n \in N. \end{aligned} \tag{33}$$

In order to measure the difference between the packet arrival rate and average service rate, the objective function of (33) can be expressed by the least-square format, that is

$$\begin{aligned}&f(n;x_n)\\ &= \underset{x_n}{\operatorname{argmin}}\ \Big\|(1+\ldots+N-n)\ln p_n + (N-n)\ln(x_n) + \ldots\\ &\qquad + (N-n-1)\ln(x_n+\alpha_n d_n)\\ &\qquad + \ln(x_n+(N-1)\alpha_n d_n) - \lambda_n\Big\|^2\\ &\text{s.t. } (N-n)x_n + (1+\ldots+N-n)\alpha_n d_n < T_n,\\ &\quad x_n > 0,\ \alpha_n > 0, \quad \forall n \in N. \end{aligned} \tag{34}$$

Expand (34) recursively beginning with x_0 as an initial conditions, After some algebraic manipulation (34) can be put in the following form

$$\begin{aligned}&\underset{x_n}{\operatorname{argmin}}\ \Big\|\sum_n k_n^1 \ln(x_n + k_n^2\alpha_n d_n) - \lambda_n\Big\|^2\\ &\text{s.t. } k_n^3 x_n + k_n^4 \alpha_n d_n < T_n,\ x_n > 0,\\ &\quad \alpha_n > 0, \quad \forall n \in N. \end{aligned} \tag{35}$$

where

$$\begin{aligned}&k_n^1 = N-n, \quad k_n^2 = N-n+1,\\ &k_n^3 = N-n, \quad k_n^4 = (1+2+\cdots+N-n+1)\end{aligned}$$

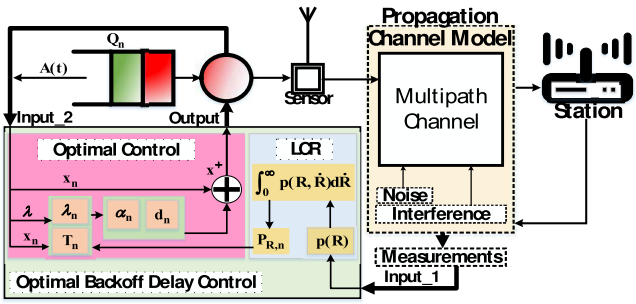

Fig. 4. Overview of the OBDC scheme.

$$\begin{aligned}\lambda_n &= \lambda - N\ln p_0 - \cdots - (N-n-1)\ln p_n,\\ T_n &= T - x_0 - x_1 - \cdots - x_{n-1}\end{aligned} \tag{36}$$

We consider the quadratic penalty method, in which the penalty terms are the squares of the constraint violation, that is

$$\begin{aligned}&\underset{x_n}{\operatorname{argmin}}\ \Big\|\sum_n k_n^1 \ln(x_n + k_n^2\alpha_n d_n) - \lambda_n\Big\|^2\\ &\qquad + \frac{c}{2}\Big\|k_n^3 x_n + k_n^4\alpha_n d_n - T_n\Big\|^2\\ &\text{s.t. } k_n^3 x_n + k_n^4 \alpha_n d_n < T_n,\\ &\quad x_n > 0, \alpha_n > 0, \quad \forall n \in N. \end{aligned} \tag{37}$$

In summary, we want to find the optimal TSN by controlling the back-off delay of the packet in the service interval. To meet this end, first, we investigate the PDF of LCR on the basis of the measured PDF of the impulse response signal through the industrial wireless channel. We refer to the obtained PDF of LCR in a given threshold at the time instant Δt as the transition probability of the proposed phase-type embedded Markov model. Then, considering the proposed semi-Markov model, we investigate the probability distribution function of the interval between the SN sets the back-off delay of the packet and the SN successfully detects an idle channel status to transmit the packet. After that, we build up the connection between the probability distribution of the back-off delay and the expected TSN by exploring their KL divergence. We find that the performance of TSN can be improved by controlling the back-off delay of the packet. In order to ensure the system stability, we minimize the KL divergence between the probability distribution of the back-off delay and the packet arrival times. Finally, we suppose that the TSN should be within a determined constraint. We build the constrained objective function based on the penalty method and replace the problem by a single function consisting of the original objective function plus one additional term for the constraint. In the next section, we will explore how to minimize the TSN by controlling the back-off delay of the packet based on (37).

IV. Optimal Back-Off Delay Control

By exploring the LCR of the industrial wireless channel, the proposed OBDC scheme iteratively decrease the packet back-off delay under the constraint of the delay limitation of the TSN. As depicted in Fig. 4, the OBDC scheme consists

Algorithm 1 Optimal Back-Off Delay Control Algorithm

Data: $H \triangleq$ positive definite symmetric matrix
$\lambda \triangleq$ average arrival rate, $P_{R,0} \triangleq$ level crossing rate
Result: TX = **ON**
$n = 0$; $\alpha_n = 0, d_n = 0, \mu_n = 1, c = 100$
Randomly Initialize $x_n = \text{rnd}[1, 2^{BE} - 1]$
Initial **CSMA/CA**
if *Channel* == ***Idle*** **then**
  TX = **ON**
end
else
  repeat
    $(k_n^1, k_n^2, k_n^3, k_n^4, \lambda_n, T_n) \leftarrow$ (36)
    $f_n = \sum_n k_n^1 \ln(x_n + k_n^2 \alpha_n d_n) - \lambda_n$, $g_n = k_n^3 x_n + k_n^4 \alpha_n d_n - T_n$
    $F_n = \|f_n\|^2 + \mu_n g_n + \frac{c}{2}\|g_n\|^2$
    $d_{n+1} \leftarrow$ (44), $\alpha_{n+1} \leftarrow$ (47), $x_{n+1} = x_n + \alpha_{n+1} d_{n+1}$
    $\mu^{n+1} = \max(c^n(d_n x_n + h_n \alpha_n d_n - T_n) + \mu^n, 0)$
    $c_{n+1} > c_n$
    $n = n + 1$
    Initial **CSMA/CA**
    if *Channel* == ***Idle*** **then**
      TX = **ON**
    end
    else
      Continue
    end
  until $n >$ *maxMacCSMAback-offs*
end

of two processing blocks: LCR and Optimal Control. There are two inputs in the OBDC scheme. One input is the PDF of the received signal which is calculated by the measurement results from the practical manufacturing environments. The other input is the combination of the current packet arrival rate and the packet back-off delay. In the LCR block, according to (2), the time-varying feature of the propagation channel is evaluated, which improves the interference tolerance capability of the scheme. After that, the transition probability $P_{R,n}$ is calculated based on the measurement results. In the Optimal Control block, all the variables in (37) including λ_n and T_n are determined based on $P_{R,n}$ and current back-off delay x_n. Moreover, new back-off delay descent direction d_n and the related step size α_n are obtained by optimizing the objective function in (37). Finally, the optimal back-off delay for next transmission round is renewed by $x_{n+1} = x_n + \alpha_{n+1} d_{n+1}$. The details of the proposed scheme is given in Alg. 1. In this section, first, we prove that quadratic barrier function in (37) is able to prevent feasible iterates from moving too close to the constraint condition of the TSN. Second, we discuss the optimality condition, find the optimal back-off delay descent direction subject to this condition, and then address how to choose the back-off delay along the direction in each step.

A. Quadratic Barrier

We provide the barrier function as quadratic-barrier method, in which quadratic terms prevents feasible iterates from moving too close to the limitation of the TSN. Convert (37) to equality constrained problem

$$\bar{F}(x_n, \mu) = \min_z F(x_n, u, \mu)$$

$$= \Big\| \sum_n k_n^1 \ln(x_n + k_n^2 \alpha_n d_n) - \lambda_n \Big\|^2 + \min_{u \geq 0} \Big\{ \mu(k_n^3 x_n + k_n^4 \alpha_n d_n - T_n + u) + \frac{c}{2} \| k_n^3 x_n + k_n^4 \alpha_n d_n - T_n + u \|^2 \Big\} \quad (38)$$

where $u \geq 0$. The constrained minimum of (38) is $u^* = \max\{0, \hat{u}\}$, where $\hat{u}$ is the unconstrained minimum with the derivative of 0.

$$0 = \nabla_u \min_z F(x_n, u, \mu)$$
$$\Rightarrow \hat{u} = -\frac{\mu}{c} - \left(k_n^3 x_n + k_n^4 \alpha_n d_n - T_n\right)$$

Thus, we have

$$k_n^3 x_n + k_n^4 \alpha_n d_n - T_n + u^* = \max\{k_n^3 x_n + k_n^4 \alpha_n d_n - T_n, -\frac{\mu}{c}\} \quad (39)$$

Substituting (39) into (38), $\bar{F}(x_n, \mu)$ can be expressed as

$$\Big\| \sum_n k_n^1 \ln(x_n + k_n^2 \alpha_n d_n) - c_n \Big\|^2 + \frac{1}{2c} \Big\{ \left[\max(c(k_n^3 x_n + k_n^4 \alpha_n d_n - T_n) + \mu, 0) \right]^2 - \mu^2 \Big\} \quad (40)$$

Taking derivatives of (40) with respect to μ, we obtain the iterative expression of the Lagrange multiplier μ^*, which is

$$\mu^{k+1} = \max(c^k(k_n^3 x_n + k_n^4 \alpha_n d_n - T_n) + \mu^k, 0) \quad (41)$$

Additionally, note that the penalty function under inequality constrained function is

$$\frac{1}{2c} \Big[\max(c(k_n^3 x_n + k_n^4 \alpha_n d_n - T_n) + \mu, 0) \Big]^2 - \frac{1}{2c}\mu^2 \quad (42)$$

Equation (42) proves that when $k_n^3 x_n + k_n^4 \alpha_n d_n$, which is the summation of all past back-off delay, is smaller than $T_n - \frac{\mu}{c}$, there is no extra punishment from the penalty function. In each system transmission round, the system should initiate x_n according to the value of $T_n - \frac{\mu}{c}$. When $k_n^3 x_n + k_n^4 \alpha_n d_n$ is larger than T_n, a large punishment is given to the objective function with a growing difference between $k_n^3 x_n + k_n^4 \alpha_n d_n$ and T_n.

B. Discussion and Integrated Solution

The OBDC scheme minimizes the TSN by addressing the objective function (37). Specifically, the back-off delay which contributes to the TSN, is obtained by adding the initial back-off delay and a proper delay step along the optimal direction. The direction is calculated by considering the quadratic approximation of (37) at the current back-off point. This quadratic approximation is subject to a necessary optimality condition which is specified by the direction. We choose the delay step size which can yield a reduction in the objective function along the obtained direction. *Proposition:* if we have $\bar{F}(x_n + \alpha d, \mu) < \bar{F}(x_n, \mu)$ over X, then

$$(x_n + \alpha d - x_n) \Delta \bar{F}(x_n, \mu) < 0, \ \forall x \in X$$

Proof: Suppose that $(x_n+\alpha d-x_n)\,\Delta\bar{F}\,(x_n,\mu)<0$ for some $x\in X$. By the mean value theorem [26], for every $\epsilon>0$ there exists an $s\in[0,1]$ such that $\bar{F}[x_n+\epsilon(x_n+\alpha d-x_n)]=\bar{F}(x_n,\mu)+\epsilon\Delta\bar{F}[x_n+s\epsilon(x_n+\alpha d-x_n)](x_n+\alpha d-x_n)$. Considering the assumption, we have for all sufficiently small $\epsilon>0$, $(x_n+\alpha d-x_n)\,\Delta\bar{F}\,(x_n,\mu)<0$ Then, it follows $\bar{F}\,(x_n+\alpha d,\mu)<\bar{F}\,(x_n,\mu)$.

This completes the proof. ■

The idea in investigating the optimal direction is to minimize the quadratic approximation of $\bar{F}$ around the point x_n with the consideration of the necessary condition $\alpha d\Delta\bar{F}(x_n,\mu)<0$ which is used to ensure $\bar{F}(x_n+\alpha d,\mu)<\bar{F}(x_n,\mu)$.

1) Back-Off Delay Descent Direction: Suppose $z-x=d$. We set $\alpha=1$ and define a quadratic function of $z-x$ with the constrained of $\bar{F}(x_n,\mu)$ as

$$\begin{aligned}\min_{z}\ &\frac{1}{2}(z-x_n)'H(z-x_n)+\bar{F}(x_n,\mu)\\&+(z-x_n)\Bigg[\frac{2k_n^1(\sum_n k_n^1\ln(x_n+k_n^2\alpha_n d_n)-\lambda_n)}{x_n+k_n^2\alpha_n d_n}\\&+\max\big(c(k_n^3x_n+k_n^4\alpha_n d_n-T_n)+\mu,0\big)cd_n\Bigg]\\\text{s.t. }&(z-x_n)\nabla\bar{F}(x_n,\mu)\le 0\end{aligned}\tag{43}$$

where we define H as a positive definite symmetric matrix to simplify the calculation complexity. Substituting (40) into (43) and taking integrative with respect to z, we have the direction as

$$\begin{aligned}d_{n+1}&=z-x_n\\&=-\frac{2k_n^1(\sum_n k_n^1\ln(x_n+k_n^2\alpha_n d_n)-\lambda_n)H^T}{(x_n+k_n^2\alpha_n d_n)HH^T}\\&\quad+\frac{\max(c(k_n^3x_n+k_n^4\alpha_n d_n-T_n)+\mu,0)cd_nH^T}{HH^T}\end{aligned}\tag{44}$$

2) Back-Off Delay Control: Given x_n and the descent direction d_{n+1}, the difference between $\bar{F}(x_n+\alpha_n d_{n+1},\mu)$ and $\bar{F}(x_n,\mu)$ is

$$\begin{aligned}&\bar{F}(x_n+\alpha_n d_{n+1},\mu)-\bar{F}(x_n,\mu)\\&\le\int_0^{\alpha_n}d'_{n+1}\nabla\bar{F}(x_n+\alpha_n d_{n+1},\mu)\mathbf{d}\alpha_n\\&\quad+\Bigg|\int_0^{\alpha_n}d'_{n+1}\big(\nabla\bar{F}(x_n+\alpha_n d_{n+1},\mu)\\&\quad-\nabla\bar{F}(x_n,\mu)\big)\mathbf{d}\alpha_n\Bigg|\\&=\alpha_n\nabla\bar{F}(x_n,\mu)d_{n+1}+\frac{1}{2}\alpha_nL_n\|d_{n+1}\|^2\end{aligned}\tag{45}$$

where d_n is the changing direction of the back-off delay at the nth transmission round. Considering the Lipschitz assumption [26], L_n is some scalar which satisfies

$$L_n\ge\frac{\bar{F}(x_n+\alpha_n d_{n+1},\mu)-\bar{F}(x_n,\mu)}{\alpha_n\|d_{n+1}\|}\tag{46}$$

Minimizing of (45) over α_n yields the back-off step size

$$\alpha_{n+1}=\frac{\big|\nabla\bar{F}(x_n,\mu)d_{n+1}\big|}{L_n\|d_{n+1}\|^2}\tag{47}$$

Combine (44) and (47), then we have $x_{n+1}=x_n+\alpha_{n+1}d_{n+1}$.

It seems that the calculation method proposed in the OBCD scheme for choosing the back-off delay is more complicated than that in conventional protocols which select the back-off delay randomly from a duration. However, it should be pointed out that, the aim of the OBDC scheme is not to exactly solve (37) with sequence results which are iteratively converged to the optimal point. Instead, we determine the back-off delay by exploring the proper back-off delay descent direction and step-size according to (37). The aim of the OBDC scheme is to take reasonable direction and step-size when we have decided the back-off delay in each transmission round. Thus, in each transmission round, the OBDC scheme only needs to update the objective function, calculate the descent direction and choose the proper back-off step-size for the direction.

V. Performance Evaluation

In this paper, we use the average TSN and deadline-meeting ratio (DMR) to evaluate the performance of the proposed OBDC scheme. We define the DMR of packet as the proportion of the packets meeting their deadline to the total packets. The variables employed in this evaluation include the LCR which refers to the probability of SNs detecting a busy channel, the deadline for packets, the number of SNs and the packet arrival rate. We evaluate the scheme by changing one variables each time while keeping the others fixed. Additionally, we design two schemes, one is called constant scheme, with constant back-off delay for all the packets, the other is exponential scheme, in which the packet service time follows an exponential distribution. We use these two schemes and the CSQC scheme in [4] as the benchmark to compare with the performance of the OBDC scheme. We evaluate the performance of the proposed OBDC scheme on OMNET++. The simulation environment is in a 100×100m area, where 10 SNs are uniformly scattered. There is one base station in the network to cover the SNs and collect the transmitted data from the SNs. A star network topology is considered and shown in Fig. 1. A channel model based on experimental data from an industrial environment is utilized. We then compare the four schemes in terms of long-term performance and the related PDF by varying the LCR of the industrial wireless channel and the threshold of delay constraint.

The channel model for industrial propagation environment reported in [28] is utilized. The model takes into account the time-varying multipath propagation conditions. A two-state Markov model is used for changing the fading rate of the channel. Denote by $n(t)$ the noise that follows zero-mean Gaussian distribution. Denote by $J(t)=\sum_{n=0}^{N-1}\sqrt{2}\beta_n e^{j\phi_n(t)}$ a group of interference signals, where β_n is the n-th interference power. Denote by $J_g(t)$ the event that the channel is distorted by interference signals and $J_b(t)$ the event that there is only noise in the wireless channel. According

TABLE I
SIMULATION SETTING

Parameter		
Notation	**Description**	**Value**
f	Frequency	**2.4GHz**
f_c	Sampling frequency	**10Hz**
T	Simulation time	**300s**
M	The number of scatters	**100**
p_t	Transmit power	Adaptive
F	Receiver noise figure	**11dBm**
B	Receiver noise bandwidth	**5MHz**
T_n	Noise temperature	**290K**
p_{01}	Transition probability from $J_g(t)$ to $J_b(t)$	**0.005**
p_{10}	Transition probability from $J_b(t)$ to $J_g(t)$	**0.1**
N	Number of interfering signals	**7**
J	Total interference power	**4dBm**
K	Ricean K-factor of multipath component	**5dBm**
η	Relative permittivity of the reflecting surface at 2.4GHz	$\mathbf{1-j802}$
n	Path-loss exponent	**1.72** [27]
σ	Shadowing variation	**3.76** [27]
γ	Adaptor factor	**0.2**

to [28], the channel is described as sum of delayed multipath components, with time-varying fading effects, expressed as $h(t) = \sum_{m=0}^{M} \alpha_m(t) \cdot \delta(t - \tau_m(t)) \cdot e^{j(2\pi f_m(t) - \phi_{D_m}(t))}$, where $\tau_m(t)$ is the delay caused by the m-th scatter at time t, α_m is the power gain factor from the m-th scatter. $\phi_{D_m}(t)$ is the phase changes caused by time-varying channel conditions. f_c is the carrier frequency and f_m is the Doppler shift at the m-th moving scatter [29]. The details of channel setting can be found in Table. I. The path loss exponent and shadowing variance are obtained from measurements at industrial environment [27]. The SNs are randomly deployed in the map and provide one-hop transmission with the BS. All the SNs initialize transmission power with 0 dB. See [28] for details on the channel modelling. The simulation results are shown as follows.

3) LCR: In this part, the performance of the OBDC scheme is evaluated in terms of PDF, average TSN and DMR by changing the LCR in the system. The number of SNs, deadline and packet arrival rate are set as 10, 20ms, 0.1, respectively. The results show that, compared with other schemes, when LCR is increased which implies that SNs can always detect a busy channel, the OBDC scheme can both achieve better performance on the influence tolerance to the channel impairments and guarantee the system delay stability for a long time. Fig. 5 shows the PDF of the TSN with different LCRs on the basis of different operation schemes. It can be seen that, in contrast to the constant and exponential schemes, the OBDC scheme can keep the TSN within $(0.1\ 0.3)$ms. This means that the OBDC scheme can control the TSN within a confidential interval. This is because the OBDC scheme optimizes the TSN by controlling the value of the next back-off delay at the optimal direction. Also note that this direction is obtained by solving (37) which is subject to the constraints composed by the summation of the past back-off delay. Then, we increase LCR by increasing the power of the received multipath signal or interference effects to increase the frequency of the SNs

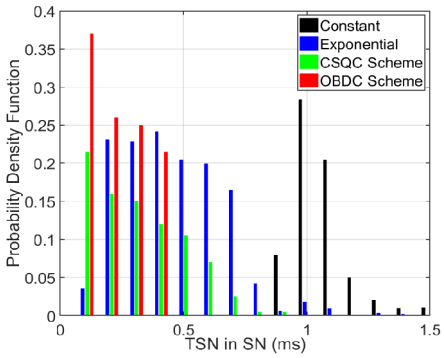

Fig. 5. PDF of TSN vs. LCR.

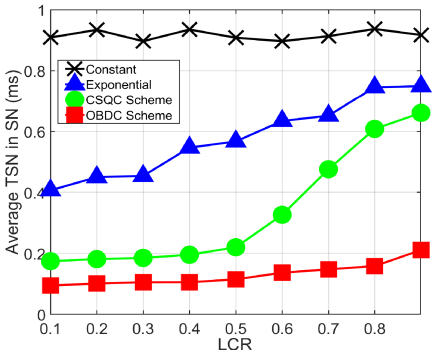

Fig. 6. Average TSN vs. LCR.

detecting a busy channel. As shown in Fig. 6, when LCR is increased, the OBDC scheme still performs better than the other schemes and keep the TSN within an acceptable range to guarantee the stability of the system. This is because, according to the objective function (37) of the OBDC scheme, increasing LCR is equivalent to decreasing the arrival rate. This does not change the descent direction of (37) but the size of the back-off delay obtained by the scheme. When LCR is increased, the OBDC scheme will calculate a larger step to achieve a better back-off delay for the packet. However, it can be seen that the average TSN will increase when SN can always detect a busy channel. Fig. 7 shows that compared with other schemes, if we set the packet deadline as 1ms, the packets which are transmitted under the OBDC scheme have a bigger chance to meet the deadline. The reason is that the OBDC scheme controls the back-off delay of each packet according to both the failure times of channel detection and the pre-configured packet deadline.

4) Deadline: In this part, the changing variable is the pre-configured packet deadline. The number of SNs, LCR and packet arrival rate are set as 10, 0.1 and 0.1, respectively. We find that compared with other schemes, when the pre-configured packet deadline is changed, the OBDC scheme can achieve better performance of TSN and system requirements of delay variance. This relationship can also be observed in Fig. 8. Fig. 9 shows that TSN increases with the increase of the pre-configured packet deadline. This is because when we increase the deadline, we enlarge the range of the inequality constraint function in (35) at the same time. Thus, it

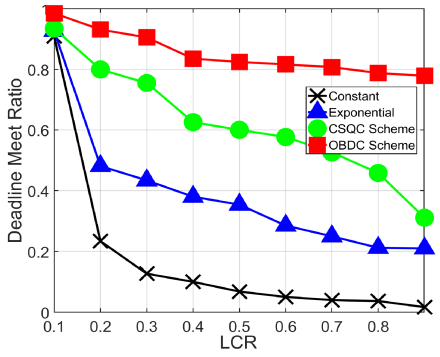

Fig. 7. DMR vs. LCR.

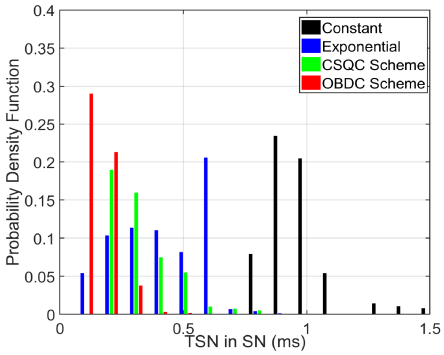

Fig. 8. PDF of TSN vs. deadline.

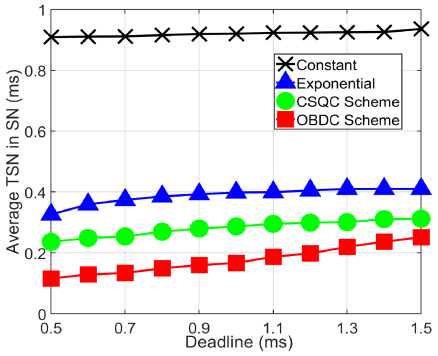

Fig. 9. Average TSN vs. deadline.

is as the same as solving the objective function (37) in a larger solution space. Since we do not consider the closed form results of (37), we need to increase the packet back-off delay along the descent direction in a larger step to find the optimal delay. Also note that the OBDC scheme performs much better than the CSQC scheme. The reason is twofold. First, the OBDC scheme is developed based on a new evaluation model which considers a uniformly distributed packet sojourn duration. It enables the OBDC scheme to precisely estimate the TSN and establish (37) to calculate the optimal back-off delay of the packet. Second, in contrast to the CSQC scheme, the OBDC scheme considers the time constraint condition in the model. This only allows the OBDC scheme to control the TSN within a pre-configured delay constraint. Fig. 10 shows that DMR is increased when the packet deadline is increased.

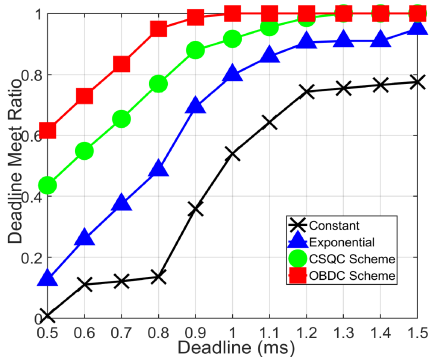

Fig. 10. DMR vs. deadline.

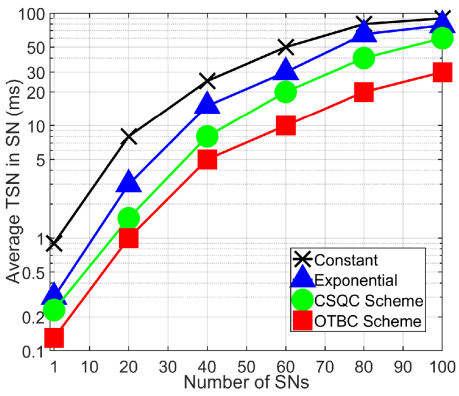

Fig. 11. Average TSN vs. number of sensor.

Obviously, compared with Fig. 9, when the pre-configured packet deadline is increased, the number of packets in SN to meet this deadline will increase.

5) Number of SN: In this part, we evaluate the average TSN and the DMR of the OBDC scheme by changing the number of SN. The LCR, deadline and packet arrival rate are set as 0.1, 20ms and 0.1, respectively. Fig. 11 shows that compared with other schemes, when the number of SN is changed, the OBDC scheme performs better in controlling the packet delay. With the increasing number of SNs, the channel contention probability will be increased. Since we consider the contention probability of SN in the objective function (37), the OBDC scheme can control the TSN according to the information on the number of SNs. In addition, since (37) is renewed constantly in each packet transmission round, the OBDC scheme can respond quickly to the sudden change of the number of SN in the wireless network and further control the TSN. Fig. 12 shows that although the DMR of the OBDC scheme is decreased when the number of SN is increasing, OBDC scheme still achieves a much better performance on TSN than all the other considered schemes.

6) Packet Arrival Rate: In this part, we change the packet arrival rate. The LCR, deadline and number of SNs are set as 0.1, 20ms and 10, respectively. Fig. 13 shows that the OBDC scheme achieves much better performance on TSN than the other three schemes. The reason is that, according to (32), we build up the objective function of the OBDC scheme by minimizing the KL divergence between the probability

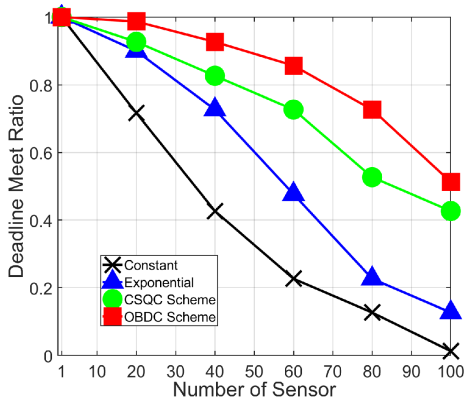

Fig. 12. DMR vs. number of sensor.

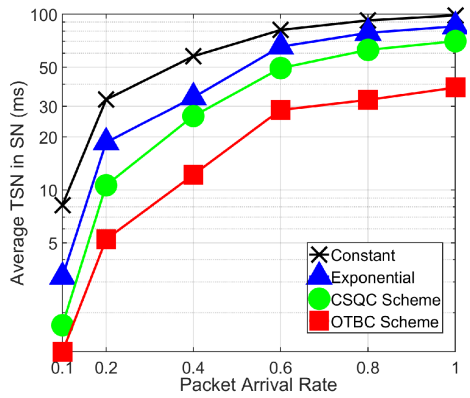

Fig. 13. Average TSN vs. packet arrival rate.

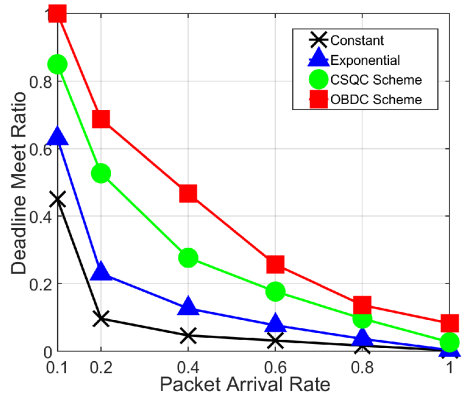

Fig. 14. DMR vs. packet arrival rate.

distribution of average packet back-off delay and the packet arrival interval which is produced by the arrival rate. Thus, in every transmission round, (37) can constantly control the TSN according to the knowledge of the packet arrival rate. Although the CSQC scheme also considers the data sampling with the instantaneous information on the channel status, it cannot renew the objective function constantly to make response to the change in each transmission round and thus fail to control the TSN. Fig. 14 shows that the DMR of the OBDC scheme is decreased when the packet arrival rate is increased.

VI. Conclusion

In this paper, we have proposed a channel-based delay minimization scheme, called OBDC scheme, for IWSNs. The simulation results show that the OBDC scheme can minimize TSN and keep the TSN within the confidential interval even if the wireless propagation channel is influenced by the noise and interference effects in the industrial environment. Moreover, by combining LCR and the proposed phase-type semi-Markov model, the OBDC scheme can react quickly to the time-varying wireless channel and find the optimal back-off delay of each packet to control the TSN when the number of SN and the LCR is changing. Furthermore, by constantly updating the objective function bound by the delay constraints in each transmission rounds, the OBDC scheme can dynamically change the back-off delay and control the TSN within an acceptable range even if the deadline of the packet is re-configured and the arrival rate of packets is increased. For the future work, we will study the average fading duration of the industrial channel model such that the sensors can predict the sampling rate and queuing state to further minimize the packet delay.

Appendix A
Proof of Level Crossing Probability

According to (1), we have

$$\begin{aligned}\sum_n x_n &= R\cos\theta - Q \\ &= I_c \\ &= \sum_n \left(p_n \cos(w_n t + \theta_n) - q_n \cos(v_n t)\right) \qquad (48)\\ \sum_n y_n &= R\sin\theta \\ &= I_s \\ &= \sum_n \left(p_n \sin(w_n t + \theta_n) - q_n \sin(v_n t)\right) \qquad (49)\end{aligned}$$

After serval modifications, we can summarize x_n and y_n as

$$x_n = x_{n,1}\cos qt - x_{n,2}\sin qt,\ \ y_n = y_{n,1}\cos qt - y_{n,2}\sin qt \qquad (50)$$

where

$$\begin{aligned}x_{n,1} &= y_{n,2} \\ &= A_c\cos[(w_n - q)t + \theta_n] + A_s\sin[(w_n - q)t + \theta_n] \\ x_{n,2} &= y_{n,1} \\ &= A_c\sin[(w_n - q)t + \theta_n] - A_s\cos[(w_n - q)t + \theta_n] \\ A_c &= p_n - g_n\cos(v_n t - w_n t - \theta_n), \\ A_s &= g_n\sin(v_n t - w_n t - \theta_n)\end{aligned}$$

Remark that the trigonometry method in Fig. 15 addresses the influence of multipath fading and interference effects to the final received signal. We combine all the components from the multipath signals and interference into the received signal, such that we can calculate the joint function of these

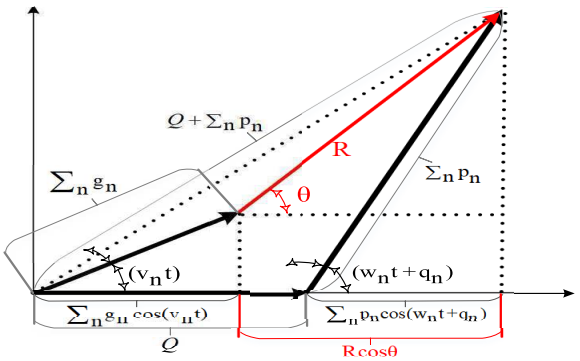

Fig. 15. Received signal $R = Q + \sum_n p_n - \sum_n g_n$.

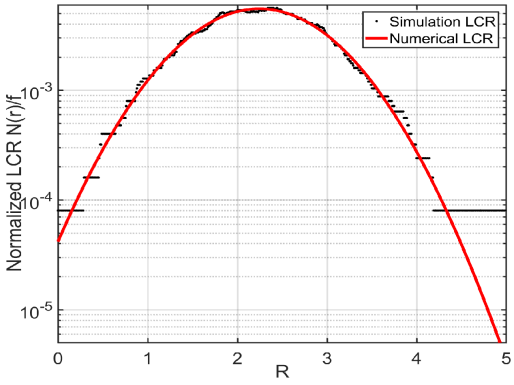

Fig. 16. Normalized LCR result numerical vs. simulation.

three components by giving the moment matrix and covariance matrix of the joint density function of R, that is

$$\boldsymbol{A} = \begin{pmatrix} I_c^2 & I_c I_s & I_c \dot{I}_c & I_c \dot{I}_s \\ I_s I_c & I_s^2 & I_s \dot{I}_c & I_s \dot{I}_s \\ \dot{I}_c I_c & \dot{I}_c I_s & \dot{I}_c^2 & \dot{I}_c \dot{I}_s \\ \dot{I}_s I_c & \dot{I}_s I_s & \dot{I}_s \dot{I}_c & \dot{I}_s^2 \end{pmatrix} \tag{51}$$

$$\boldsymbol{M} = \begin{pmatrix} a_0 & a_1 & 0 & a_4 \\ a_1 & a_0 & -a_4 & 0 \\ 0 & -a_4 & a_2 & a_3 \\ a_4 & 0 & a_3 & a_2 \end{pmatrix} \tag{52}$$

where

$$\begin{aligned} a_0 &= \frac{1}{2n}\sum_n p_n^2 + g_n^2, \ a_1 = \frac{1}{2n}\sum_n p_n^2, \\ a_2 &= \frac{1}{2n}\sum_n g_n^2 (v_n - w_n)^2 + (p_n^2 + g_n^2)(w_n - q)^2 \\ a_3 &= \frac{1}{2n}\sum_n p_n^2 (w_n - q), \quad a_4 = \frac{1}{2n}\sum_n g_n^2 (v_n - w_n) \end{aligned} \tag{53}$$

Let M^{-1} be the inverse matrix of M, that is $\boldsymbol{M}^{-1} = \frac{\text{adj}(\boldsymbol{M})}{\det(\boldsymbol{M})}$, where $\text{adj}(\boldsymbol{M})$ is the adjugate of matrix $\boldsymbol{M}$ and $\det(\boldsymbol{M})$ is the matrix determinant. The substitutions

$$\begin{aligned} I_c &= R\cos\theta - Q, \ \dot{I}_c = \dot{R}\cos\theta - R\sin\dot{\theta}, \\ I_s &= R\sin\theta, \ \dot{I}_s = \dot{R}\sin\theta + R\cos\dot{\theta}, \\ dI_c dI_s d\dot{I}_c d\dot{I}_s &= R^2 dR d\dot{R} d\theta d\dot{\theta} \end{aligned} \tag{54}$$

enable us to write the probability density function of R, $\dot{R}$, θ and $\dot{\theta}$ as

$$\begin{aligned} &p(R, \dot{R}, \theta, \dot{\theta}) \\ &= \frac{R^2}{4\pi^2 \det(\boldsymbol{M})} \exp\left(-\frac{1}{2\det(\boldsymbol{M})} \sum_{i,j} A_{i,j} \text{adj}(M_{i,j}) \right) \end{aligned} \tag{55}$$

where R ranges from 0 to ∞, θ from $-\pi$ to π, $\dot{R}$ and $\dot{\theta}$ is from $-\infty$ to ∞. The PDF for R and $\dot{R}$ is obtained by integrating (55) with respect to θ and $\dot{\theta}$ over their respective ranges, that is

$$p(R, \dot{R}) = \frac{R^2}{4\pi^2 \det(\boldsymbol{M})} \int_0^{2\pi} \int_{-\infty}^{\infty} \exp\left(-\frac{1}{2\det(\boldsymbol{M})} \cdot \sum_{i,j} A_{i,j} \text{adj}(M_{i,j}) \right) d\theta d\dot{\theta} \tag{56}$$

where

$$\begin{aligned} &\sum_{i,j} A_{i,j} \text{adj}(M_{i,j}) \\ &= 2s_1 s_2(-a_3 a_0^2 + a_3 a_1^2 + a_1 a_4^2) \\ &\quad -s_2^2(-a_2 a_0^2 + a_0 a_4^2 + a_2 a_1^2) \\ &\quad -s_3^2(-a_0 a_2^2 + a_2 a_4^2 + a_0 a_3^2) \\ &\quad -s_1^2(-a_2 a_0^2 + a_0 a_4^2 + a_2 a_1^2) \\ &\quad -R^2 \sin\theta^2(-a_0 a_2^2 + a_2 a_4^2 + a_0 a_3^2) \\ &\quad -2s_2 s_3(a_4^3 - a_0 a_2 a_4 + a_1 a_3 a_4) \\ &\quad -2s_1 s_3(a_0 a_3 a - 4 - a_1 a_2 a_4) \\ &\quad -2Rs_1 \sin\theta(a_4^3 - a_0 a_2 a - 4 + a_1 a_3 a_4) \\ &\quad -2Rs_2 \sin\theta(a_0 a_3 a_4 - a_1 a_2 a_4) \\ &\quad -2Rs_3 \sin\theta(-a_1 a_2^2 + a_1 a_3^2 + a_3 a_4^2) \end{aligned} \tag{57}$$

and

$$\begin{aligned} s_1 &= \dot{R}\cos\theta - R\dot{\theta}\sin\theta, \quad s_2 = \dot{R}\sin\theta + R\dot{\theta}\sin\theta, \\ s_3 &= Q - R\cos\theta \end{aligned}$$

Consider some definite integrals of exponential function, that is

$$\begin{aligned} &\int_{-\infty}^{\infty} e^{-ax^2} e^{-2bx} dx = \sqrt{\frac{\pi}{a}} e^{\frac{b^2}{a}}, \\ &\int_0^{2\pi} e^{x\cos\theta + y\sin\theta} d\theta = 2\pi I_0\left(\sqrt{x^2 + y^2}\right) \end{aligned} \tag{58}$$

After some algebraic manipulation, we find that the expression of LCR can be summarized as

$$\begin{aligned} N_r(R) &= \frac{2\pi^{-1/2}}{\sqrt{\det(M)(2A + B)}} \\ &\quad \times \begin{bmatrix} \text{Probability Density of} \\ \text{envelop at the value } R \end{bmatrix} \end{aligned} \tag{59}$$

where

$$\begin{aligned} A &= -a_3a_0^2 + a_3a_1^2 + a_1a_4^2, \\ B &= -a_2a_0^2 + a_0a_4^2 + a_2a_1^2 \\ \det(M) &= a_0^2a_2^2 - a_0^2a_3^2 - 2a_0a_2a_4^2 - a_1^2a_2^2 + a_1^2a_3^2 + a_4^4 \\ &\quad +2a_1a_3a_4^2 \end{aligned}$$

And a_0, a_1, a_2, a_3, a_4 can be obtained from (53). The PDF of the received signal has been proved in [4]. Fig. 16 confirms that LCR, which has been obtained from the simulation, are identical to the analytic expressions describing in (2).

REFERENCES

[1] J. Dai, J. Liu, Y. Shi, S. Zhang, and J. Ma, "Analytical modeling of resource allocation in D2D overlaying multihop multichannel uplink cellular networks," *IEEE Trans. Veh. Technol.*, vol. 66, no. 8, pp. 6633–6644, Aug. 2017.

[2] W. Sun, J. Liu, Y. Yue, and H. Zhang, "Double auction-based resource allocation for mobile edge computing in industrial Internet of Things," *IEEE Trans. Ind. Informat.*, vol. 14, no. 10, pp. 4692–4701, Oct. 2018.

[3] M. Cheffena, "Industrial wireless communications over the millimeter wave spectrum: Opportunities and challenges," *IEEE Commun. Mag.*, vol. 54, no. 9, pp. 66–72, Sep. 2019.

[4] Q. Li, K. Zhang, M. Cheffena, and X. Shen, "Channel-based sampling rate and queuing state control in delay-constraint industrial WSNs," in *Proc. IEEE Global Commun. Conf. (GLOBECOM)*, Dec. 2017, pp. 1–6.

[5] T. Olofsson, A. Ahlén, and M. Gidlund, "Modeling of the fading statistics of wireless sensor network channels in industrial environments," *IEEE Trans. Signal Process.*, vol. 64, no. 12, pp. 3021–3034, Mar. 2016.

[6] Q. Wang, D. O. Wu, and P. Fan, "Delay-constrained optimal link scheduling in wireless sensor networks," *IEEE Trans. Veh. Technol.*, vol. 59, no. 9, pp. 4564–4577, Nov. 2010.

[7] J. Liu, H. Nishiyama, N. Kato, and J. Guo, "On the outage probability of device-to-device-communication-enabled multichannel cellular networks: An RSS-threshold-based perspective," *IEEE J. Sel. Areas Commun.*, vol. 34, no. 1, pp. 163–175, Jan. 2016.

[8] M. F. Uddin, C. Rosenberg, W. Zhuang, P. Mitran, and A. Girard, "Joint routing and medium access control in fixed random access wireless multihop networks," *IEEE/ACM Trans. Netw.*, vol. 22, no. 1, pp. 80–93, Feb. 2014.

[9] L. Musavian and S. Aissa, "Effective capacity of delay-constrained cognitive radio in Nakagami fading channels," *IEEE Trans. Wireless Commun.*, vol. 9, no. 3, pp. 1054–1062, Mar. 2010.

[10] Y. Cui, V. K. N. Lau, R. Wang, H. Huang, and S. Zhang, "A survey on delay-aware resource control for wireless systems—Large deviation theory, stochastic Lyapunov drift, and distributed stochastic learning," *IEEE Trans. Inf. Theory*, vol. 58, no. 3, pp. 1677–1701, Mar. 2012.

[11] J. Chen and V. Lau, "Delay analysis of max-weight queue algorithm for time-varying wireless ad hoc networks—Control theoretical approach," *IEEE Trans. Signal Process.*, vol. 61, no. 1, pp. 99–108, Jan. 2013.

[12] L. Lei, Y. Kuang, X. S. Shen, K. Yang, J. Qiao, and Z. Zhong, "Optimal reliability in energy harvesting industrial wireless sensor networks," *IEEE Trans. Wireless Commun.*, vol. 15, no. 8, pp. 5399–5413, Aug. 2016.

[13] D. Qiao and J. Han, "Achievable throughput of energy harvesting fading multiple-access channels under statistical QoS constraints," *IEEE Trans. Wireless Commun.*, vol. 17, no. 5, pp. 2906–2917, May 2018.

[14] Y. Yun and Y. Xia, "Maximizing the lifetime of wireless sensor networks with mobile Sink in delay-tolerant applications," *IEEE Trans. Mobile Comput.*, vol. 9, no. 9, pp. 1308–1318, Sep. 2010.

[15] M. J. Neely, "Delay-based network utility maximization," *IEEE/ACM Trans. Netw.*, vol. 21, no. 1, pp. 41–54, Feb. 2013.

[16] M. J. Neely and S. Supittayapornpong, "Dynamic Markov decision policies for delay constrained wireless scheduling," *IEEE Trans. Autom. Control*, vol. 58, no. 8, pp. 1948–1961, Aug. 2013.

[17] L. Lei, Y. Kuang, N. Cheng, X. S. Shen, Z. Zhong, and C. Lin, "Delay-optimal dynamic mode selection and resource allocation in device-to-device communications—Part I: Optimal policy," *IEEE Trans. Veh. Technol.*, vol. 65, no. 5, pp. 3474–3490, May 2016.

[18] Y. Yun, Y. Xia, B. Behdani, and J. C. Smith, "Distributed algorithm for lifetime maximization in a delay-tolerant wireless sensor network with a mobile sink," *IEEE Trans. Mobile Comput.*, vol. 12, no. 10, pp. 1920–1930, Oct. 2013.

[19] Q. Li and M. Cheffena, "Hidden channel learning-based optimal backoff control in industrial WSNs," *IEEE Trans. Wireless Commun.*, to be published.

[20] C. Buratti, "Performance analysis of IEEE 802.15.4 beacon-enabled mode," *IEEE Trans. Veh. Technol.*, vol. 59, no. 4, pp. 2031–2045, May 2010.

[21] *IEEE Standard for Local and Metropolitan Area Networks—Part 15.4: Low-Rate Wireless Personal Area Networks (LR-WPANs)*, IEEE Standard 802.15.4-2011, Sep. 2011, pp. 1–314.

[22] L. Kleinrock, *Queueing System: Theory*, vol. 1. Hoboken, NJ, USA: Wiley, 1975.

[23] J. Ren, Y. Zhang, R. Deng, N. Zhang, D. Zhang, and X. Shen, "Joint channel access and sampling rate control in energy harvesting cognitive radio sensor networks," *IEEE Trans. Emerg. Topics Comput.*, vol. 7, no. 1, pp. 149–161, Jan./Mar. 2019.

[24] L. Lei *et al.*, "Stochastic delay analysis for train control services in next-generation high-speed railway communications system," *IEEE Trans. Intell. Transp. Syst.*, vol. 17, no. 1, pp. 48–64, Jan. 2016.

[25] R. Deng, Y. Zhang, S. He, J. Chen, and X. Shen, "Maximizing network utility of rechargeable sensor networks with spatiotemporally coupled constraints," *IEEE J. Sel. Areas Commun.*, vol. 34, no. 5, pp. 1307–1319, May 2016.

[26] D. P. Bertsekas, *Nonlinear Programming*. Nashua, NH, USA: Athena Scientific, 1999.

[27] Y. Ai, M. Cheffena, and Q. Li, "Radio frequency measurements and capacity analysis for industrial indoor environments," in *Proc. 9th Eur. Conf. Antennas Propag. (EuCAP)*, Apr. 2015, pp. 1–5.

[28] M. Cheffena, "Industrial wireless sensor networks: Channel modeling and performance evaluation," *EURASIP J. Wireless Commun. Netw.*, vol. 2012, no. 1, p. 297, Dec. 2012.

[29] Q. Li, K. Zhang, M. Cheffena, and X. S. Shen, "Exploiting dispersive power gain and delay spread for Sybil detection in industrial wsns," in *Proc. IEEE (ICCC)*, Jul. 2016, pp. 1–6.

Qihao Li (M'16) received the M.Sc. degree in information and communication technology from the University of Agder, Norway, in 2014, and the Ph.D. degree from the Norwegian University of Science and Technology (NTNU), Norway, in 2019. In 2016, he was a Visiting Researcher with the Department of Electrical and Computer Engineering, University of Waterloo, Waterloo, ON, Canada. His current research interests include industrial wireless sensor networks, optimal control and optimization, and wireless network security and localization.

Ning Zhang (M'15–SM'18) received the Ph.D. degree from the University of Waterloo, Canada, in 2015. After that, he was a Post-Doctoral Research Fellow with the University of Waterloo and the University of Toronto, Canada. Since 2017, he has been an Assistant Professor at Texas A&M University-Corpus Christi, USA. His current research interests include wireless communication and networking, mobile edge computing, machine learning, and physical-layer security. He was the recipient of the best paper awards from the IEEE Globecom in 2014, the IEEE WCSP in 2015, the Journal of Communications and Information Networks in 2018, the IEEE ICC in 2019, the IEEE TAOS Technical Committee in 2019, and the IEEE ICCC in 2019. He was the Workshop Chair for MobiEdge'18 (in conjunction with the IEEE WiMob 2018), CoopEdge'18 (in conjunction with IEEE EDGE 2018), and 5G&NTN'19 (in conjunction with IEEE EDGE 2019). He serves as an Associate Editor for the IEEE INTERNET OF THINGS JOURNAL, the IEEE TRANSACTIONS ON COGNITIVE COMMUNICATIONS AND NETWORKING, IEEE ACCESS, *IET Communications*, and *Vehicular Communications* (Elsevier) and an Area Editor for the *Encyclopedia of Wireless Networks* (Springer). He also serves/served as a Guest Editor for several international journals, such as the IEEE WIRELESS COMMUNICATIONS, the IEEE TRANSACTIONS ON COGNITIVE COMMUNICATIONS AND NETWORKING, IEEE ACCESS, and *IET Communications*.

Michael Cheffena received the M.Sc. degree in electronics and computer technology from the University of Oslo, Norway, in 2005, and the Ph.D. degree from the Norwegian University of Science and Technology (NTNU), Trondheim, in 2008. In 2007, he was a Visiting Researcher with the Communications Research Center, Canada. From 2009 to 2010, he conducted a Post-Doctoral Study at the University Graduate Center at Kjeller, Norway, and at the French Space Agency, Toulouse. He is currently a Full Professor with NTNU, Gjøvik. His research interests include modeling and prediction of propagation radio channels, signal processing, and medium access control (MAC) protocol design.

Xuemin (Sherman) Shen (M'97–SM'02–F'09) received the Ph.D. degree in electrical engineering from Rutgers University, New Brunswick, NJ, USA, in 1990. He is currently a University Professor with the Department of Electrical and Computer Engineering, University of Waterloo, Waterloo, ON, Canada. His research interests focus on resource management in interconnected wireless/wired networks, wireless network security, social networks, smart grid, and vehicular ad hoc and sensor networks. He is a fellow of the Engineering Institute of Canada, the Canadian Academy of Engineering, and the Royal Society of Canada. He was the recipient of the Premiers Research Excellence Award (PREA) from the Province of Ontario, Canada, in 2003, the Outstanding Performance Award from the University of Waterloo in 2004, 2007, 2010, and 2014, the Excellent Graduate Supervision Award from the University of Waterloo in 2006, the Joseph LoCicero Award and the Education Award from the IEEE Communications Society in 2015 and 2017, respectively, and the James Evans Avant Garde Award from the IEEE Vehicular Technology Society in 2018. He served as the Technical Program Committee Chair/Co-Chair for the IEEE Globecom16, the IEEE Infocom14, the IEEE VTC10 Fall, and the IEEE Globecom07, the Symposia Chair for the IEEE ICC10, the Tutorial Chair for the IEEE VTC11 Spring, and the Chair for the IEEE Communications Society Technical Committee on Wireless Communications and P2P Communications and Networking. He is a registered Professional Engineer of Ontario, Canada, and a Distinguished Lecturer of the IEEE Vehicular Technology Society and Communications Society. He is also the Vice President on Publications of the IEEE Communications Society. He is the Editor-in-Chief of the IEEE INTERNET OF THINGS JOURNAL.